Genetic Vaccines and Therapy

BioMed Central

Research

Open Access

# Recombinant adeno-associated virus type 2-mediated gene delivery into the *Rpe65*$^{-/-}$ knockout mouse eye results in limited rescue

Chooi-May Lai†[1], Meaghan JT Yu†[2], Meliha Brankov[2], Nigel L Barnett[3], Xiaohuai Zhou[4], T Michael Redmond[5], Kristina Narfstrom[6] and P Elizabeth Rakoczy*[1]

Address: [1]Centre for Ophthalmology and Visual Science, The University of Western Australia, Perth, Western Australia, 6009, Australia, [2]Department of Molecular Ophthalmology, Lions Eye Institute and The University of Western Australia, Perth, Western Australia, 6009, Australia, [3]Vision Touch and Hearing Research Centre, School of Biomedical Sciences, University of Queensland, Brisbane, Queensland, 4072, Australia, [4]Virus Core Facility, Gene Therapy Center, University of North Carolina, North Carolina, 27599, USA, [5]Laboratory of Retinal Cell and Molecular Biology, National Eye Institute, National Institutes of Health, Bethesda, Maryland, 20892, USA and [6]Vision Science Group, Department of Veterinary Medicine and Surgery, College of Veterinary Medicine, University of Missouri-Columbia, Columbia, Missouri, 65211, USA

Email: Chooi-May Lai - mlai@cyllene.uwa.edu.au; Meaghan JT Yu - meaghan@cyllene.uwa.edu.au; Meliha Brankov - melabra@cyllene.uwa.edu.au; Nigel L Barnett - n.barnett@uq.edu.au; Xiaohuai Zhou - xzhou@med.unc.edu; T Michael Redmond - redmond@helix.nih.gov; Kristina Narfstrom - narfstromk@missouri.edu; P Elizabeth Rakoczy* - rakoczy@cyllene.uwa.edu.au

* Corresponding author †Equal contributors

Published: 27 April 2004

*Genetic Vaccines and Therapy* 2004, **2**:3

Received: 23 December 2003
Accepted: 27 April 2004

This article is available from: http://www.gvt-journal.com/content/2/1/3



## Abstract

**Background:** Leber's congenital amaurosis (LCA) is a severe form of retinal dystrophy. Mutations in the RPE65 gene, which is abundantly expressed in retinal pigment epithelial (RPE) cells, account for approximately 10–15% of LCA cases. In this study we used the high turnover, and rapid breeding and maturation time of the *Rpe65*$^{-/-}$ knockout mice to assess the efficacy of using rAAV-mediated gene therapy to replace the disrupted RPE65 gene. The potential for rAAV-mediated gene treatment of LCA was then analyzed by determining the pattern of RPE65 expression, the physiological and histological effects that it produced, and any improvement in visual function.

**Methods:** rAAV.RPE65 was injected into the subretinal space of *Rpe65*$^{-/-}$ knockout mice and control mice. Histological and immunohistological analyses were performed to evaluate any rescue of photoreceptors and to determine longevity and pattern of transgene expression. Electron microscopy was used to examine ultrastructural changes, and electroretinography was used to measure changes in visual function following rAAV.RPE65 injection.

**Results:** rAAV-mediated RPE65 expression was detected for up to 18 months post injection. The delivery of rAAV.RPE65 to *Rpe65*$^{-/-}$ mouse retinas resulted in a transient improvement in the maximum b-wave amplitude under both scotopic and photopic conditions (76% and 59% increase above uninjected controls, respectively) but no changes were observed in a-wave amplitude. However, this increase in b-wave amplitude was not accompanied by any slow down in photoreceptor degeneration or apoptotic cell death. Delivery of rAAV.RPE65 also resulted in a decrease in retinyl ester lipid droplets and an increase in short wavelength cone opsin-positive cells, suggesting that the recovery of RPE65 expression has long-term benefits for retinal health.

**Conclusion:** This work demonstrated the potential benefits of using the *Rpe65*$^{-/-}$ mice to study the effects and mechanism of rAAV.RPE65-mediated gene delivery into the retina. Although the functional recovery in this model was not as robust as in the dog model, these experiments provided important clues about the long-term physiological benefits of restoration of RPE65 expression in the retina.

## Background

Leber's congenital amaurosis (LCA) comprises a heterogeneous group of retinal dystrophies. It is characterized by severe visual loss from birth, nystagmus, poor pupillary reflexes, retinal pigmentary or atrophic changes, and markedly diminished electroretinography (ERG) responses [1-3]. Mutations in Rpe65, a gene that is predominantly expressed in retinal pigment epithelial (RPE) cells, cause about 10–15% of all LCA cases [4-6]. RPE65 is abundantly expressed in RPE cells, where it is involved in regenerating the visual pigment chromophore,11-*cis* retinal, from all-*trans* retinol, the latter being a product of photoreceptor phototransduction [7-9]. This recycling process, known as the visual cycle, is central to vision as 11-*cis* retinal is used by the photoreceptors to convert light photons into neuronal signals [8,9].

*In vivo* analyses, using the spontaneous-mutation RPE65 dog and *Rpe65*$^{-/-}$ mouse models of LCA, have shown that loss of RPE65 leads to severely depressed electroretinography (ERG) responses [7,10-14] and behavioral impairments indicative of diminished vision [15,16]. In addition, morphological studies have shown that the lack of RPE65 is associated with a gradual degeneration of the photoreceptor cells and a characteristic accumulation of lipid inclusion bodies in the RPE cells, the latter from an over accumulation of intermediary visual cycle pigments such as retinyl esters [7,17].

The animal models of LCA not only provide an insight into the nature of the associated disease, but have also been used to test potential therapies for its treatment [16,18-23]. A number of recent studies, using both the RPE65 dog and *Rpe65*$^{-/-}$ mouse models, have demonstrated that there is some promise for a future treatment of LCA being developed. Assessment of both RPE transplantation and oral/intraperitoneal administration of 9-*cis* retinal in the *Rpe65*$^{-/-}$ mouse have both shown that improved ERG responses can be produced [18-20]. In addition, it is well established that the subretinal delivery and expression of normal, non-mutated RPE65 in the RPE cells of RPE65 dogs results in functional recovery of vision, as seen by improvements in both ERG and behavioral responses, the latter indicative of the presence of limited vision [16,21-23]. The functional recovery produced in the RPE65 dog model was generated by using recombinant adenoassociated virus (rAAV) to deliver and express normal, non-mutated RPE65 cDNA [16,22,23]. The use of rAAV-mediated gene therapy has attracted much interest as it demonstrated a number of characteristics that may be beneficial in a clinical setting. These include a low immune response; long-term transgene expression providing minimal surgical intervention; and localized, specific transgene expression which minimizes the potential of unwanted, systemic side effects.

We wished to further examine the suitability of rAAV-mediated gene therapy for treating LCA. In this study, we used the high turnover, and rapid breeding and maturation time of mice to assess the efficacy of using rAAV-mediated gene therapy to replace the missing RPE65 gene in the *Rpe65*$^{-/-}$ knockout strain. The potential for rAAV-mediated gene treatment of LCA was then analyzed by determining the pattern of RPE65 expression and the physiological and histological effects that it produced.

## Methods

### *Virus preparation*

The *EcoRI*/*KpnI* fragment of mouse RPE65 cDNA (GenBank Accession Number: NM_029987) was inserted into the pCI mammalian expression vector (Promega Corp., WI, USA) to produce a pCI.RPE65 subclone. A 3800 bp cassette, consisting of the RPE65 cDNA flanked by a 5' human cytomegalovirus (CMV) promoter and a 3' SV40 late polyadenylation signal sequence, was removed from pCI.RPE65 by *BglII*/*BspHI* restriction enzyme digest. This cassette was then inserted between the inverted terminal repeats of the serotype 2 rAAV plasmid pSSV9 [24]. The insertion was achieved by blunt end ligation of the 3800 bp CMV.RPE65 cassette with the large fragment of pSSV9 following *XbaI* digestion [24]. The identity of the pSSV9.CMV.RPE65 vector was confirmed by restriction enzyme analysis. The expression of RPE65 protein from pSSV9.CMV.RPE65 was confirmed by western blot analysis of pSSV9.CMV.RPE65-transfected, human embryonic kidney (HEK) 293 cells using a rabbit anti-RPE65 polyclonal antibody [25].

pSSV9.CMV.RPE65, AAV helper (Ad8) and adenovirus helper plasmid DNA were co-transfected into HEK293 cells. The excision and replication of the resultant rAAV.RPE65 DNA was verified by Hirt analysis [26]. Upon successful verification, cesium chloride gradient purified pSSV9.CMV.RPE65 DNA was either co-transfected with Ad8 and adenovirus helper plasmid DNA into HEK293 cells and the resulting virus (rAAV.RPE65) purified by cesium chloride gradient density as previously described [24], or was sent to the Vector Core Facility (University of North Carolina, NC, USA) for large-scale virus production, where the virus (rAAV.RPE65.1) was purified using iodixanol gradient followed by heparin-affinity chromatography according to published methods [27]. The titers of rAAV.RPE65 and rAAV.RPE65.1 were both $6 \times 10^{13}$ particles/ml.

### *Animals*

All procedures were approved by the University of Western Australia Animal Experimentation Ethics Committee and were in compliance with the Association for Research in Vision and Ophthalmology Statement for the Use of Animals in Ophthalmic and Vision Research. Mice were

housed in cages in rooms maintained at constant temperature (22°C) and humidity (50%) and with a 12:12 hr light-dark cycle. Food (Glen Forest Rodent Chow, Australia) and water were given *ad libitum*.

### *Subretinal injection of* Rpe65$^{-/-}$ *mice*

*Rpe65*$^{-/-}$ mice were anesthetized by intraperitoneal injection of ketamine (30 mg/kg) and xylazine (8 mg/kg), and their pupils dilated with topical application of a mixture containing 2.5% phenylephrine hydrochloride and 1% tropicamide (Alcon, Australia). The conjunctiva was cut and the sclera exposed. A shelving puncture of the sclera was made with a 30-gauge needle. A 32-gauge needle attached to a 5 μl Hamilton syringe was passed tangentially through the site of the sclera puncture under an operating microscope. A 1 μl solution containing $6 \times 10^{10}$ particles of rAAV.RPE65 or rAAV.RPE65.1 was then delivered into the subretinal space of the mouse eye, the diameter of which is about 3.5 mm. Successful delivery of virus into the subretinal space was confirmed by the presence of a 1 to 1.3 mm diameter circular bleb when examined by indirect ophthalmoscopy (approximately 30% of the retinal area). The needle was kept in the subretinal space for 1 min, and then withdrawn gently. Finally, a layer of antibiotic ointment was applied to the injected eye. Additional *Rpe65*$^{-/-}$ mice were injected with 1 μl of the control construct rAAV.GFP. All mice used in this study were injected upon reaching maturity, at 3 weeks of age.

### *Electroretinography*

rAAV.RPE65-injected and uninjected *Rpe65*$^{-/-}$ mice were analyzed by electroretinography (ERG) at 1–2 mo (n = 15 rAAV.RPE65-injected, n = 10 uninjected), 7 mo (n = 12 rAAV.RPE65-injected, n = 4 uninjected) and 11 mo (n = 12 rAAV.RPE65-injected, n = 6 uninjected) post-injection. Following dark-adaptation of the mice, full-field scotopic flash ERGs were recorded. The mice were anesthetized as described earlier and maintained at 37°C with a homeothermic electric blanket. Their pupils were dilated with 0.5% tropicamide (Alcon) and the cornea was protected with carmellose sodium (Celluvisc, Allergan, Australia). The ERG was recorded between a platinum electrode touching the cornea and a reference electrode in the pinna. A ground electrode was attached to the mouse's back. The flash stimulus was presented by a xenon strobe light placed 0.3 m in front of the mouse. Four consecutive responses were amplified and averaged using a MacLab/2e bioamplifier/data recorder running "Scope" software (ADInstruments, NSW, Australia). The interstimulus interval was increased from 30 sec (dimmest flash) to 5 min (brightest flash). Stimulus-response characteristics were generated by attenuating the maximum flash intensity (1.52 log cd s/m$^2$) with neutral density filters over a range of 3 log units. After the final scotopic recording, the animals were light adapted for 10 min using a background light of 1.4 log cd/m$^2$ and photopic ERGs obtained. The a-wave amplitude was measured from the baseline to the trough of the a-wave response and the b-wave amplitude was measured from the trough of the a-wave to the peak of the b-wave. Data were expressed as the mean wave amplitude ± standard error of the mean (SEM; μVolts). Two-way repeated measures analysis of variance (ANOVA) was performed on log transformed data to compare the responses from the rAAV.RPE65-injected and uninjected *Rpe65*$^{-/-}$ retinas. A *post-hoc* Bonferroni test was used to isolate significant differences ($P < 0.05$) between rAAV.RPE65-injected and uninjected *Rpe65*$^{-/-}$ mice responses at each stimulus intensity. All mice were subjected to the same conditions for ERG measurements.

### *Histological analysis*

rAAV.RPE65-injected, age-matched uninjected *Rpe65*$^{-/-}$ mice and age-matched control C57BL/6J mice were euthanased at various time points post-injection, and their eyes enucleated and fixed in 10% neutral buffered formalin for 2.5 hr. The eyes were then washed in PBS before being placed in 70% ethanol and embedded in paraffin, with care being taken to orientate the eyes so that the injection site was at a known and consistent location. Serial sections (5 μm) were cut on a Reichert-Jung 2040 microtome (Leica Microsytems, Australia), mounted on silanated glass slides, deparaffinized and rehydrated. All analyses that were performed using these eyes were carried out on sections from the region corresponding to the injection site.

For histological analysis and quantification, the sections were stained with hematoxylin and eosin, and the number of photoreceptor cells counted. Average cell numbers for each retina were established by counting the number of cells in a 100 μm section of the outer nuclear layer (using an eyepiece graticule and viewing the stained section with a 100X oil-immersion lens). Digital images of the outer nuclear layer of each section were recorded. Between three and five 100 μm regions within the subretinal bleb from each section were selected for counting. Care was taken to avoid the outer quarter to third of the retina where the retinal layers became thinner. Counts were made every 30–50 sections (150–250 μm) such that 15–20 counts were made per eye. The mean of these counts was then calculated to give an average number of photoreceptors per 100 μm for each eye. The counting was performed by 3 independent observers who were not given the identity of the samples.

### *Immunohistochemical analysis*

Serial sections from rAAV.RPE65-injected and uninjected *Rpe65*$^{-/-}$ eyes were rehydrated through graded alcohols, and then bleached by incubation in 0.25% potassium permanganate for 20 min followed by 1% oxalic acid for 5

min [28]. The sections were rinsed several times in Tris buffer (50 mM, pH 7.2) containing 1% NaCl, then blocked in 10% normal goat serum for 1 hr. The sections were incubated at 4°C overnight with a rabbit anti-RPE65 antibody [25], rinsed three times in Tris buffer and then incubated for 2 hr at room temperature with alkaline phosphatase-conjugated, goat anti-rabbit IgG (1:100, Gibco Invitrogen, CA, USA). Immunodetection was carried out using SIGMA FAST Red TR/Naphthol AS-MX (Sigma Chemical Co., MO, USA) chromogen for 10–15 min, resulting in the formation of a red/pink precipitate. The sections were counterstained lightly with Meyer's hematoxylin and mounted in an aqueous mounting medium for analysis.

For flatmount immunohistochemistry, eyes were enucleated and the injection site was marked with indelible ink and then fixed whole for 30 min in 4% paraformaldehyde. The anterior segment of each eye was removed and the neuroretina separated from the sclera-choroid-RPE layers. The separated layers were placed in separate wells of a 96-well plate and blocked with 10% normal rabbit serum at room temperature for 1 hr. The layers were then incubated overnight at 4°C with primary antibodies, rabbit anti-RPE65 antibody and rabbit anti-short wavelength cone (SWC) opsin antibody, washed with Tris-buffered saline (TBS) and incubated for 2 hr at 4°C with goat anti-rabbit IgG conjugated with FITC (fluorescein isothiocyanate; Sigma Chemical Co.). After 3 washes in TBS, radial cuts were made to the neuroretina and the sclera-choroid-RPE layers which were mounted separately on slides with GVA mounting solution (Zymed, CA, USA) and coverslipped prior to examination. Areas within the injection subretinal bleb in rAAV.RPE65-injected *Rpe65*$^{-/-}$ mice or the equivalent location in C57BL/6J and uninjected *Rpe65*$^{-/-}$ mice were examined by fluorescence microscopy. The number of SWC opsin-positive photoreceptors was counted in five 100 μm$^2$ areas within the subretinal bleb and the results analyzed and graphed.

#### *Apoptosis detection assay and analysis*

rAAV.RPE65-injected (n = 2), age-matched uninjected (n = 2) *Rpe65*$^{-/-}$, and age-matched C57BL/6J control mice were euthanased at 7 mo post-injection (8 mo of age) and their eyes enucleated, processed and sectioned as described previously. An Apoptosis detection assay was performed on these sections using the Dead End™ Colorimetric TUNEL Systems (Promega Corp.). The assay was performed as described in the manufacturer's instructions. When complete, the sections were counterstained with 0.5% methyl green for 10 min, briefly washed in water then 1-butanol, dehydrated with xylene, and mounted with DePeX mounting medium (BDH Laboratory Supplies, England, UK). Images of the outer nuclear layer were captured with an Olympus DP-7 digital camera (Olympus, NY, USA) mounted on a light microscope (Olympus BX60) using a 100X oil immersion lens. The relative level of apoptosis was then determined by expressing the number of TUNEL-positive nuclei as a percentage of the total nuclei over a 60 μm region of the retina. Three to five 60 μm regions were counted from each section, depending on the size of section, with care being taken to avoid the outer, thinning quarter of the retinas.

#### *Electron microscopy of the RPE layer of injected* Rpe65$^{-/-}$ *mice*

rAAV.RPE65-injected and uninjected eyes from *Rpe65*$^{-/-}$ mice at 20 mo post-injection (21 mo of age) were first perfused with fixative (2.5% glutaraldehyde in cacodylate buffer, pH 7.4), then enucleated and fixed for a further 24 hr in fixative at 4°C. Following careful removal of the cornea and lens, the tissues covering the injection site and outside the injection site were trimmed into 1 mm$^3$ blocks and re-immersed into fresh fixative for a further 24 hr at 4°C. After post-fixing in 1% osmium tetroxide, the tissues were processed for transmission electron microscopy (TEM) by conventional methods and embedded in Araldite. Semi-thin sections (1 μm) were stained with 0.5% toluidine blue in 5% borax and examined with a light microscope. After selecting the areas of interest, the blocks were trimmed under a dissecting microscope. Ultra-thin sections (70 nm) were then prepared on an ultramicrotome (LKB Nova, Sweden), stained with Reynolds lead citrate and examined in a Philips 410LS Transmission Electron Microscope at an accelerating voltage of 80 kV.

## Results

#### *rAAV-mediated gene delivery to the* Rpe65$^{-/-}$ *mouse retina*

The presence of RPE65 expression following subretinal injection of rAAV.RPE65 and rAAV.RPE65.1 was monitored by immunohistochemistry using a rabbit anti-RPE65 antibody. The efficiency and specificity of the RPE65 antibody was confirmed using retinal sections from C57BL/6J and uninjected *Rpe65*$^{-/-}$ mice. RPE65 immunoreactivity was readily detectable in the cytoplasm of RPE cells in C57BL/6J mice (data not shown), but was completely absent from those of uninjected *Rpe65*$^{-/-}$ mice (Fig. 1B). No RPE65 immunoreactivity was seen in the photoreceptor layers of either C57BL/6J or uninjected *Rpe65*$^{-/-}$ mouse retinas.

In a preliminary study, *Rpe65*$^{-/-}$ mice were injected with either rAAV.RPE65 or rAAV.RPE65.1. Analysis of RPE/choroid and retina flatmounts of rAAV.RPE65-injected *Rpe65*$^{-/-}$ mice showed that the area of RPE65 expression covered approximately 30% of the surface of the RPE/choroid flatmounts (corresponding to the size of the bleb created) with no RPE65 expression present in the flatmounted neuroretina. The RPE65 expression appeared contiguous within the injection area, although some

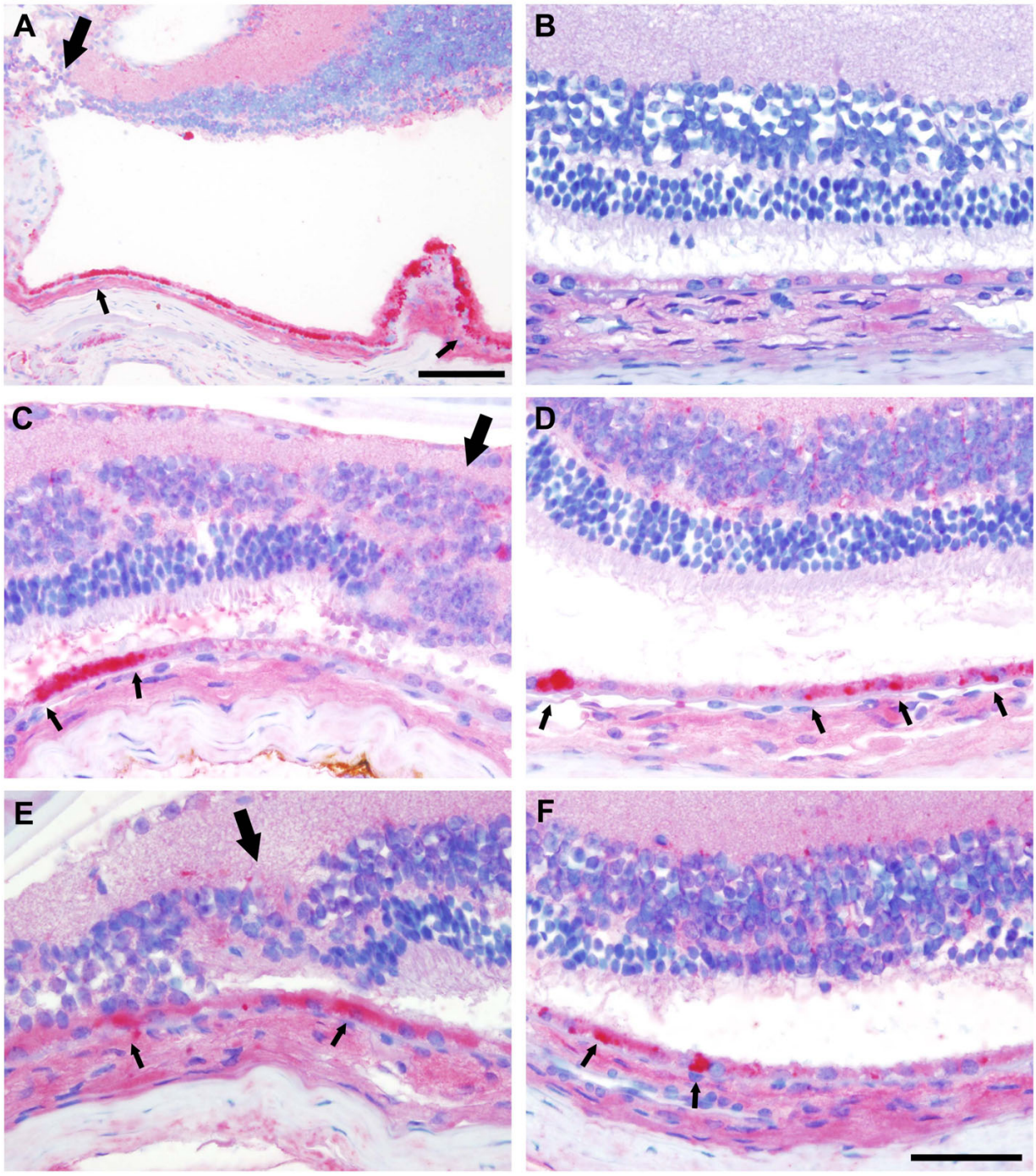


**Figure 1**
**RPE65-positive immunohistochemical labelling in the retinas of *Rpe65*$^{-/-}$ mice after injection with rAAV.RPE65**
Labeling in the retinal pigment epithelium is seen at 7 mo post-injection **(A)**. The signal continues for some distance (more than 600 μm) away from the injection site. This labeling is not seen in the uninjected, age-matched control *Rpe65*$^{-/-}$ mouse (**B**). At 11 mo post-injection positive labeling is seen both close to (**C**), and more distant from (400 μm, **D**), the injection site (**C**) although the signal is more discrete. This pattern of labeling near to **(E)** and distant from (>300 μm, **F**) the injection site persists at 18 mo post-injection (**E**, **F**). Scale bar: **A** = 100 μm; **B-F** = 50 μm. Small arrows point to positively labeled cells, large arrows point to injection site.

small, scattered areas with no signal were seen (data not shown). In contrast, in rAAV-RPE65.1-injected *Rpe65*$^{-/-}$ mice, RPE65 expression was not only present in the RPE/choroid flatmounts (again in an area of approximately 30% of the retina), but was also present in the neuroretina flatmounts where more RPE65-immunostained cells were detected. The RPE65 expression in both the RPE/choroids and neuroretina flatmounts of the rAAV-RPE65.1 injected eyes was weaker, and appeared more dispersed, probably due to the fewer number of cells transduced when compared to rAAV.RPE65-injected RPE/choroids flatmounts (data not shown). On the basis that rAAV.RPE65 was more efficient in transducing RPE cells,, and in order to target transduction of RPE cells only, subsequent studies were conducted using rAAV.RPE65.

A histological analysis of RPE65 immunoreactivity in the rAAV.RPE65-injected mice over time demonstrated that strong RPE65 positive RPE cells were visible from the injection site to up to 300–600 μm away, but still within the bleb created, at 1–2 mo (data not shown), 7 mo (Fig. 1A), 11 mo (Fig. 1C and 1D) and 18 mo (Fig. 1E and 1F) post-injection. However, the extent of RPE65 expression appeared to decrease at the latest time point. No RPE65 immunoreactivity was seen in either uninjected, age-matched control *Rpe65*$^{-/-}$ mice, or *Rpe65*$^{-/-}$ mice injected with the control rAAV.GFP construct (data not shown). There was no evidence of infiltrating immune cells in any of the eyes examined.

### *Electroretinography*

ERG analysis of *Rpe65*$^{-/-}$ mice showed an improvement in the response of rAAV.RPE65-injected animals compared with uninjected, age-matched controls. A comparison of scotopic and photopic ERG responses from injected and uninjected mice is presented in Fig. 2. At 1–2 mo post-rAAV.RPE65 injection, an increase in the ERG b-wave amplitude was apparent (Fig. 2A and 2B, upper trace). A two-way repeated measures ANOVA of the stimulus-response characteristics (Fig. 3) demonstrated a significant ($P < 0.001$) difference in the scotopic b-wave amplitude between the control and rAAV.RPE65-injected mice. *Post-hoc* Bonferroni tests revealed a significant ($P < 0.005$) increase of the scotopic b-wave at all flash intensities above -0.9 log neutral density units (Fig. 3B). There was also a significant interaction between stimulus intensity and rAAV.RPE65-injection in the photopic b-wave amplitude ($P < 0.05$). The *post-hoc* Bonferroni tests also revealed a significant ($P < 0.05$) increase of the photopic b-wave at the brightest flash intensities (Fig. 3B). No statistically significant improvement in a-wave amplitude was seen at this time point (Fig. 3A, $P > 0.05$). At 7 mo and 11 mo post-injection, no differences were found in the ERG a-wave (Fig. 2B and 2C) or b-wave amplitudes (Fig. 2B,2C, 3C and 3D) recorded from rAAV.RPE65-injected mouse eyes when compared with responses recorded from uninjected, age-matched controls under either scotopic or photopic conditions. Additional rAAV.GFP-injected *Rpe65*$^{-/-}$ control mice showed ERG signals equivalent to those of uninjected controls (data not shown).

### *Morphological effects of rAAV.RPE65 injection in* Rpe65$^{-/-}$ *mouse retinas*

Histological analysis of the retinas of uninjected *Rpe65*$^{-/-}$ mice showed a slow, progressive degeneration of photoreceptors. In brief, at the early age of 1–2 mo, the retinas of uninjected *Rpe65*$^{-/-}$ mice appeared normal, except for the less organized appearance of the photoreceptor outer segments (Fig. 4A). The outer nuclear layer of uninjected *Rpe65*$^{-/-}$ mice aged 6–12 mo were visibly thinner and the outer segments appeared highly disorganized when compared to age-matched C57BL/6J controls. At 12 mo and older (Fig. 4B), the difference in the outer nuclear layer thickness was very significant when compared to age-matched C57BL/6J mice (Fig. 4C) and by 21 mo of age, the outer nuclear layer was completely absent (data not shown). The morphologic difference was quantified by counting the number of photoreceptor nuclei in the eyes of uninjected *Rpe65*$^{-/-}$ mice at 2, 5, 7, 11, 17 and 24 mo post-injection and comparing them to those of age-matched C57BL/6J mice. A statistically significant decrease ($P < 0.05$, Student's t-test) in photoreceptor number was obtained for uninjected *Rpe65*$^{-/-}$ mice older than 3 mo (Fig. 4D), reflecting the progressive loss of photoreceptor cells in these mice. Subsequent comparison of rAAV.RPE65-injected with age-matched, uninjected control *Rpe65*$^{-/-}$ mice indicated that no statistically significant difference in the number of photoreceptors around the injection site was seen at any of the time points (Fig. 4D; $P > 0.05$, Student's t-test), suggesting that there was no photoreceptor rescue or slow down in photoreceptor loss following rAAV.RPE65 injection. The lack of photoreceptor rescue was reflected by the lack of difference in the number of apoptotic cells in rAAV.RPE65-injected eyes of *Rpe65*$^{-/-}$ mice (Fig. 5A) when compared to the contralateral uninjected eyes (Fig. 5B). At 7 mo post-injection (8 mo of age), the number of apoptotic cells in both the uninjected and rAAV.RPE65-injected *Rpe65*$^{-/-}$ appeared higher than those in age-matched C57BL/6J controls (Fig. 5C). Analysis of the 60 μm regions of uninjected and rAAV.RPE65-injected *Rpe65*$^{-/-}$ eyes at 7 mo post injection (8 mo of age) showed that 5.8 ± 1.9% and 2.7 ± 1.7%, respectively, of the remaining photoreceptors were apoptotic ($P > 0.01$, Student's t-test, Fig. 5D).

Electron microscopy of rAAV.RPE65-injected and uninjected *Rpe65*$^{-/-}$ mouse eyes at 20 mo post injection (21 mo of age) revealed the presence of retinyl ester lipid droplets that are characteristic of *Rpe65*$^{-/-}$ mice [7]. However, a direct comparison of the RPE in the rAAV.RPE65-injected

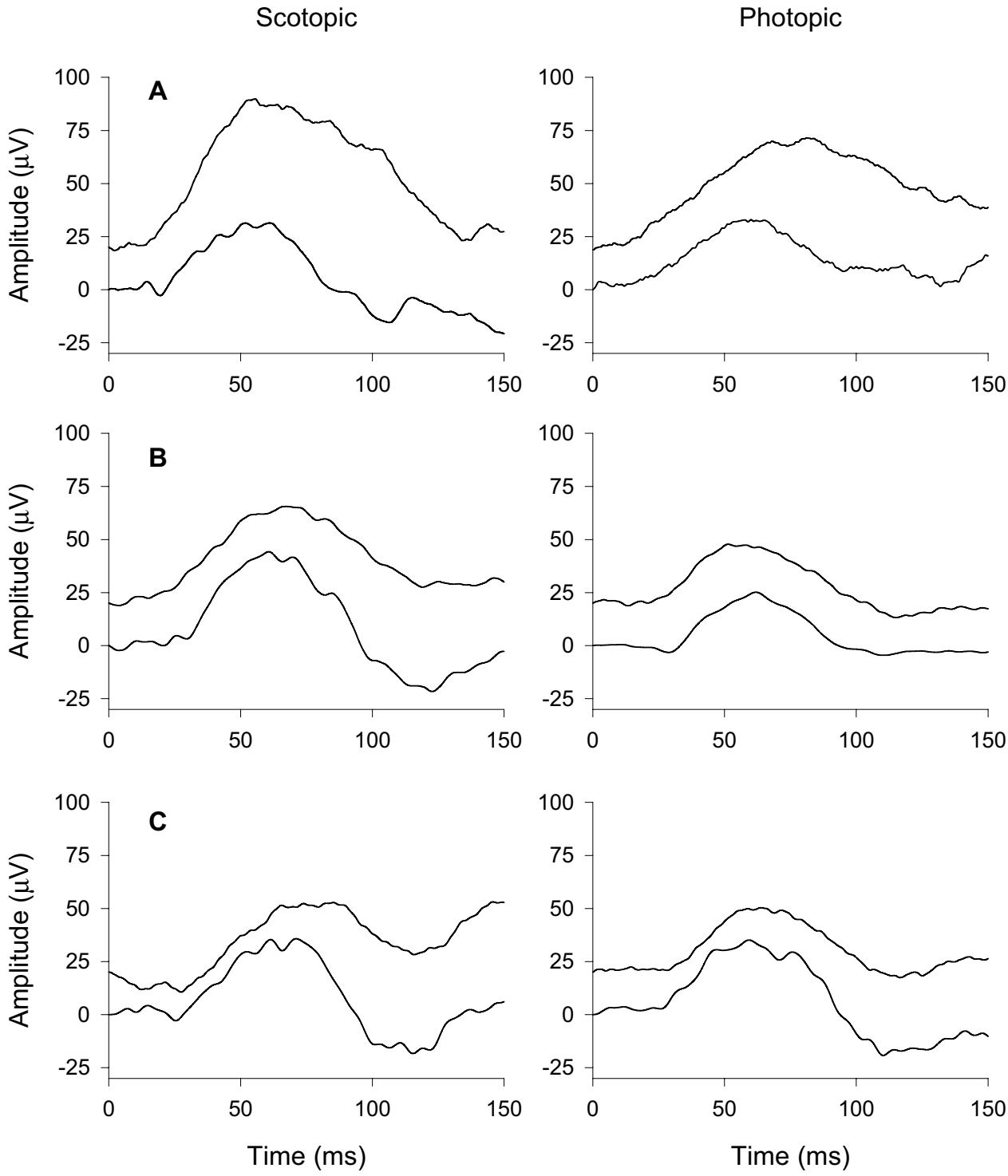


**Figure 2**
**Representative ERG responses recorded from rAAV.RPE65 injected and uninjected *Rpe65*$^{-/-}$ miceover time**
*Rpe65*$^{-/-}$ mice at 1–2 mo **(A)**, 7 mo **(B)** and 11 mo **(C)** post-injection. Each panel shows representative responses from rAAV.RPE65-injected (upper traces) and age-matched, uninjected control (lower traces) mice recorded under scotopic (left panels) or photopic (right panels) conditions.

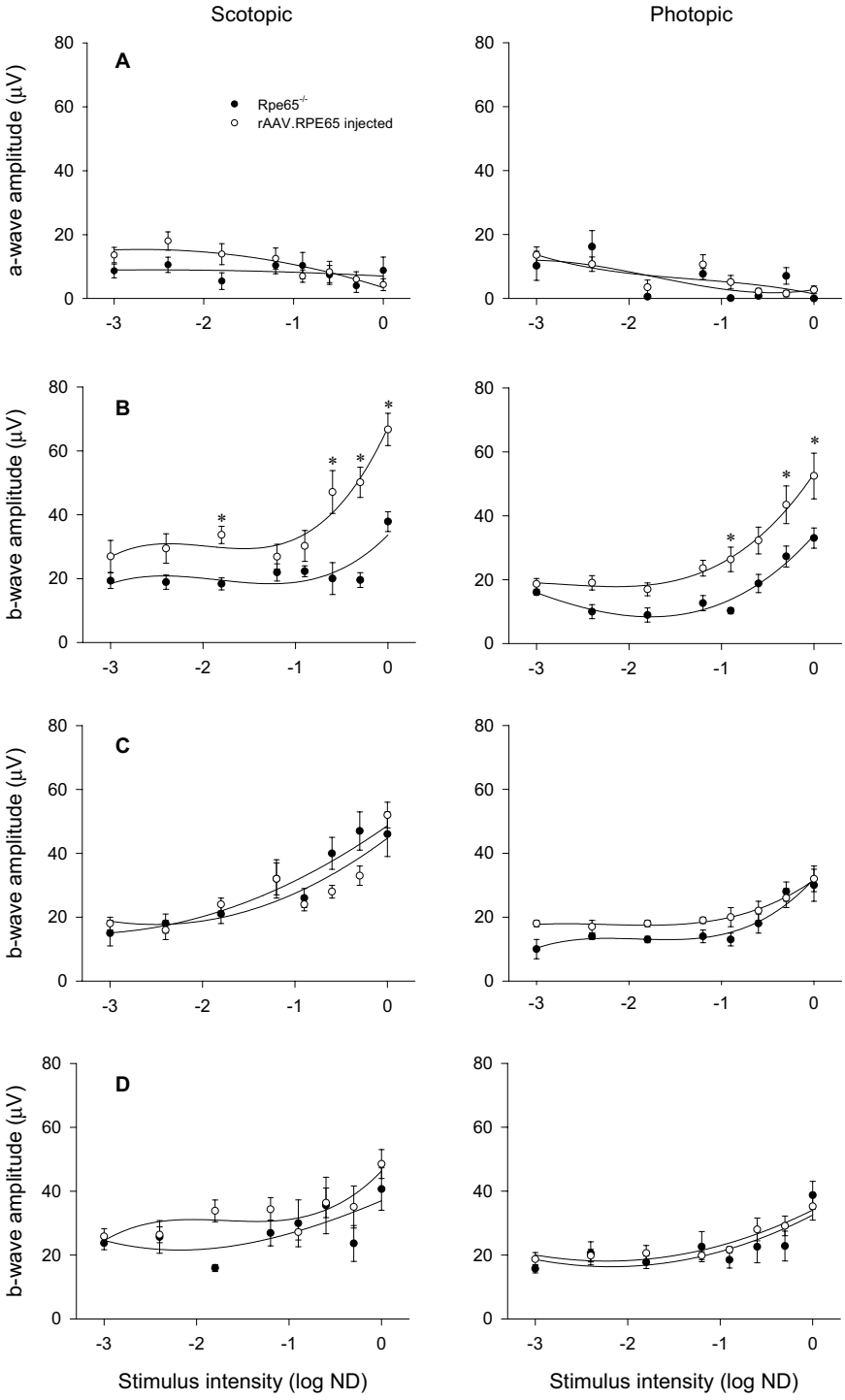


**Figure 3**

**Intensity response characteristics of scotopic and photopic ERG** Intensity response characteristics of scotopic (left panel) and photopic (right panel) ERGs recorded from rAAV.RPE65 injected (o) and age-matched, uninjected control (•) *Rpe65*$^{-/-}$ mice. Intensity response characteristics of the ERG a-waves **(A)** and b-waves **(B)** at 1–2 mo post-injection (n = 15 rAAV.RPE65 injected, n = 10 uninjected). Intensity response characteristics of the ERG b-waves at 7 mo (**C**, n = 12 rAAV.RPE65-injected, n = 4 uninjected) and 11 mo (**D**, n = 12 rAAV.RPE65 injected, n = 6 uninjected) post-injection. Data are mean values ± SEM. * = $P < 0.05$.

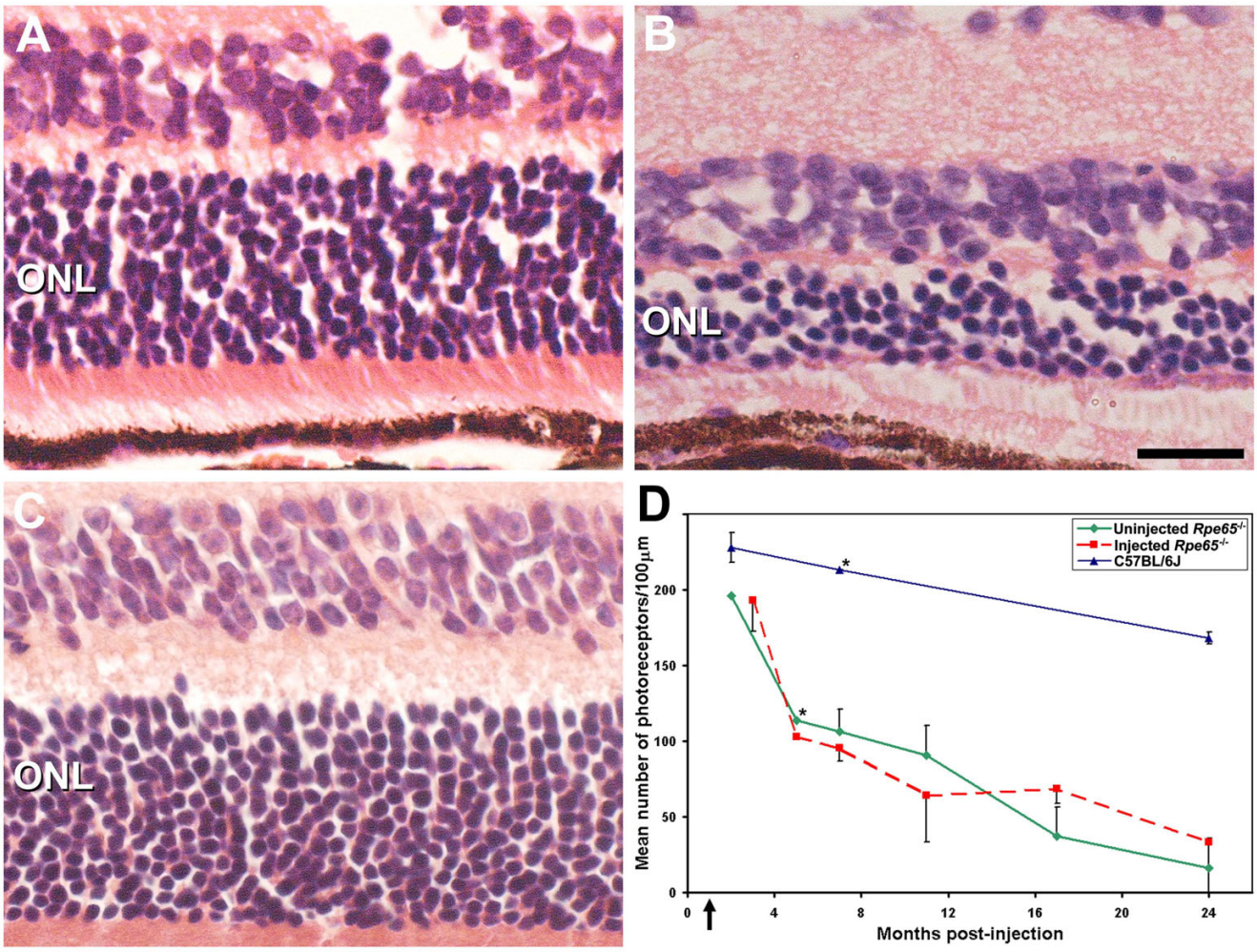


**Figure 4**
**Comparisons of photoreceptor numbers** Photomicrographs of theouter retina of a 1 mo uninjected *Rpe65*$^{-/-}$ mouse (**A**), a 14 mo injected *Rpe65*$^{-/-}$ mouse (**B**) and a 14 mo C57BL/6J mouse (**C**). (**D**) Graphical presentation of the mean number of cells per 100 μm length of the outer nuclear layer (ONL) of C57BL/6J (▲), uninjected *Rpe65*$^{-/-}$ (◆) and rAAV.RPE65 injected *Rpe65*$^{-/-}$ (') at the various ages shown. All points are calculated from the cell numbers averaged over 3 animals unless indicated (*n = 1). Arrow indicates time of injection. Scale bar: **A-C** = 20 μm.

mice (Fig. 6A) with the uninjected, age-matched control (Fig. 6B) showed a striking difference between the amounts of lipid inclusions present in these eyes. In contrast, electron microscopy of sections taken from outside the subretinal bleb of rAAV.RPE65-injected eyes showed no difference between the numbers of lipid inclusions when compared to sections from uninjected eyes (data not shown). In addition to the reduction in numbers of lipid droplets, the layer of basal infoldings was also thinner in rAAV.RPE65-injected eyes (Fig. 6A and 6B).

Immunostaining using the anti-SWC opsin antibody demonstrated the presence of SWC opsin-positive cells scattered throughout the flatmounted neuroretinas of 8 month old C57BL/6J mice (Fig. 7A). The number of SWC opsin-positive cells was significantly lower in uninjected *Rpe65*$^{-/-}$ mouse retinas, with only a small number of SWC opsin-positive cells being seen in the neuroretinas of either 3 week (Fig. 7B) or 3 month old *Rpe65*$^{-/-}$ mice (data not shown). By 8 months of age no SWC opsin-positive cells were visible in the neuroretinas of uninjected *Rpe65*$^{-/-}$ mice (Fig. 7C). Examination of flatmounted neuroretinas of 8-month-old rAAV.RPE65-injected *Rpe65*$^{-/-}$ mice

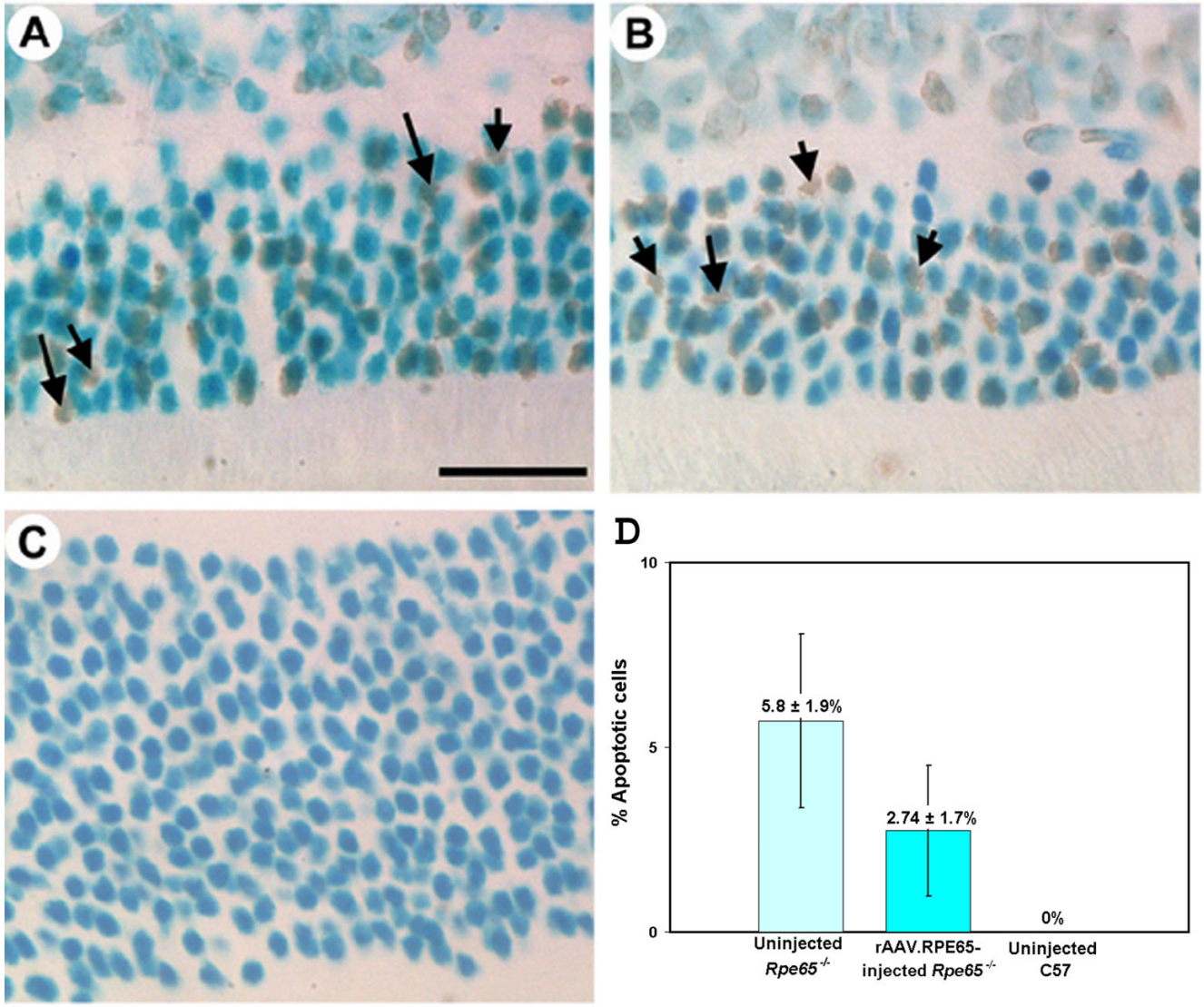


**Figure 5**

**Comparison of apoptotic cells numbers** Photomicrographs of the outer nuclear layer of 8 mo uninjected *Rpe65*$^{-/-}$ (**A**), rAAV.RPE65 injected *Rpe65*$^{-/-}$ (**B**) and C57BL/6J mice (**C**) stained for apoptotic nuclei (**arrows**). (**D**) Graphical presentation of the percentage of photoreceptor nuclei that are apoptotic in uninjected *Rpe65*$^{-/-}$, rAAV.RPE65-injected *Rpe65*$^{-/-}$ and uninjected C57BL/6J mice. Apoptotic and total photoreceptor nuclei were counted along 60 μm lengths of the outer nuclear layer of mice at 7 mo post-injection (8 mo of age). Average total photoreceptor counts: uninjected *Rpe65*$^{-/-}$ = 106.8 ± 22.9, rAAV.RPE65 injected *Rpe65*$^{-/-}$ = 134 ± 30.3, uninjected C57 = 213.5 ± 3.3. All data are mean ± S.D. Scale bar: **A-C** = 20 μm.

revealed the presence of numerous SWC opsin-positive cells in an area coinciding with the subretinal bleb and, at a higher density, around the injection site (Fig. 7D). Counting and analysis of the number of SWC opsin-positive cells in the C57BL/6J control (n = 5), uninjected *Rpe65*$^{-/-}$ mice (n = 5) and rAAV.RPE65-injected *Rpe65*$^{-/-}$ eyes (n = 5) showed that the reappearance of the SWC opsin-positive cells in rAAV.RPE65-injected *Rpe65*$^{-/-}$ mice was significant, reaching up to 50% of that seen in age-matched C57BL/6J mice (Fig. 7E).

## Discussion

We report here the results from our study examining the effects of rAAV-mediated RPE65 expression in the retinas of *Rpe65*$^{-/-}$ mice. Subretinal injection with rAAV.RPE65 purified by cesium chloride density gradient resulted in

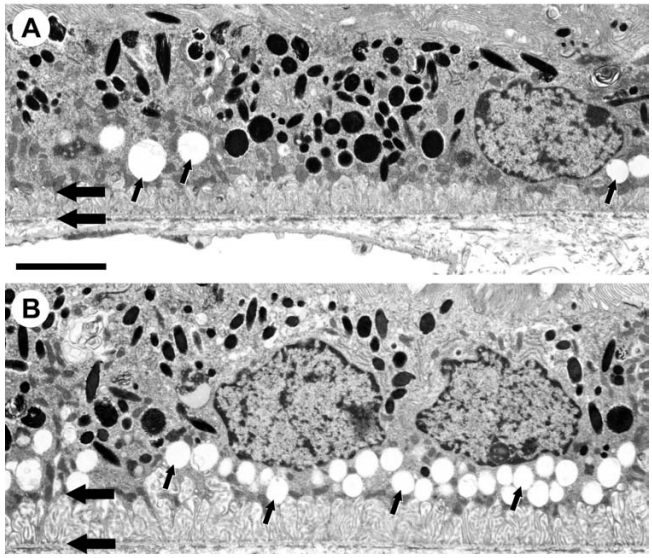


**Figure 6**
**Electron micrograph of injected and uninjected *Rpe65*$^{-/-}$ mouse retina** Electron micrograph of the RPE of an rAAV.RPE65-injected *Rpe65*$^{-/-}$ mouse at 20 mo post injection (**A**) and an age-matched, uninjected *Rpe65*$^{-/-}$ control (21 mo of age; **B**). The injected animal shows an accumulation of retinyl ester lipid droplets in the RPE layer (**small arrows**) that is not as prevalent as that in the uninjected control. The layer of basal infoldings was also thinner in the injected mouse (**large arrows**). Scale bar = 5 μm.

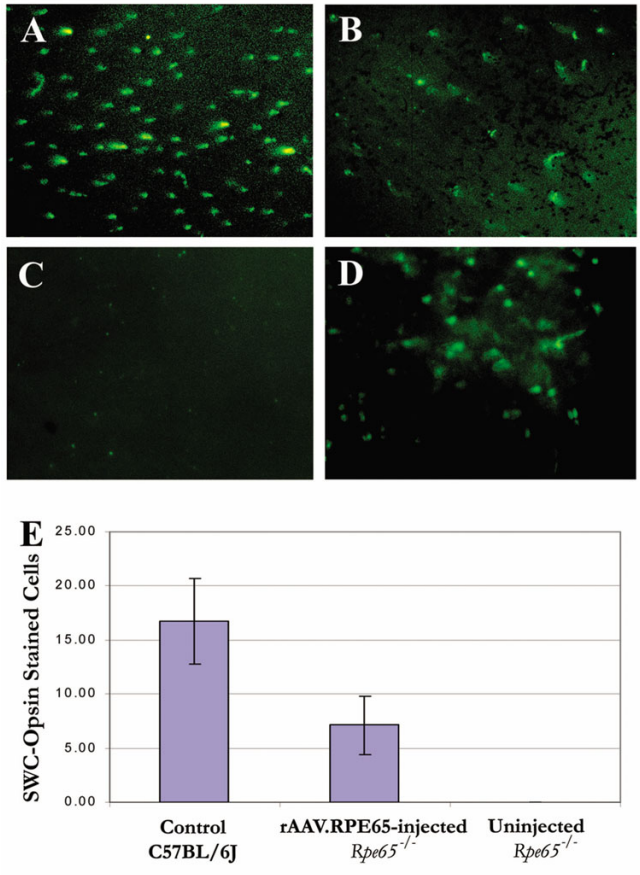


**Figure 7**
**Comparison of short wavelength cone opsin-positive cells** Photomicrographs (×40) of flatmounted neuroretinas stained for SWC opsin in an 8 mo C57BL/6J (**A**), a 3 wk uninjected *Rpe65*$^{-/-}$(**B**), an 8 mo *Rpe65*$^{-/-}$ (**C**) and an 8 mo rAAV.RPE65-injected *Rpe65*$^{-/-}$ (**D**) mouse. (**E**) Graphical presentation of the mean number of SWC opsin-positive cells per 100 μm$^2$ calculated for 8 mo C57BL/6J, rAAV.RPE65-injected and uninjected *Rpe65*$^{-/-}$ mice.

transduction of approximately 30% of the retina and produced long-term, detectable RPE65 protein expression (up to 18 mo post-injection when the experiment was terminated) in the RPE cells within the subretinal bleb of *Rpe65*$^{-/-}$ knockout mice. The longevity of this RPE65 expression agrees with previous studies where rAAV.GFP reporter gene constructs gave long-term detectable GFP signals in a variety of animals [24,29-32]. In agreement with previous rAAV.GFP research, the levels and extent of RPE65 expression from the rAAV.RPE65 injection appeared to decrease at the later time points [31]. At this stage the reason for this decrease in transgene expression is unclear. The reduction of RPE65 expression could be due to the protein not being recognized as self, but this is unlikely as there was no evidence of any infiltrating immune cells in the injected eyes. It could also be due to silencing mechanisms, such as promoter silencing [33,34] or transgene silencing [35,36], or might be due to the lack of integration [37]. Further work would be required to confirm or disprove these suggestions, the conclusions of which are important if rAAV is to be used for mediating long-term transgene expression.

Following subretinal injection the most common sites of transgene expression have been the RPE and photoreceptors cells. The extent and relative ratio of the transduction level in these two cells types tends to vary depending on factors such as the method of virus purification [31,38] and the virus serotype being used [39]. Consistent with results using rAAV.GFP [31,38], the expression of RPE65 following injection with cesium chloride density gradient purified rAAV.RPE65 was only in the RPE cells, with no expression being visible in the photoreceptors. Our laboratory has examined a number of possible contributing factors [31,38], but the precise reason for these differences has yet to be elucidated.

Although rAAV.RPE65 was delivered to an area covering 30% of the *Rpe65*$^{-/-}$ mouse retina, pan-retinal ERG responses (responses over the entire retina) were measured. Under this circumstance, the finding of an improved ERG response in rAAV.RPE65-injected *Rpe65*$^{-/-}$ mice is of great importance for the future treatment of LCA as it suggests a partial restoration of visual function. The delivery of rAAV.RPE65 to the *Rpe65*$^{-/-}$ mouse retinas resulted in improvements in the maximum b-wave amplitude under both scotopic (76% increase above uninjected controls) and photopic (59% increase above uninjected controls) conditions. However, the increase in b-wave magnitude was only seen at the initial early 1–2 mo post-injection time point of the study. The ability of rAAV.RPE65 delivery to *Rpe65*$^{-/-}$ mouse retinas to restore visual function, though limited and transient, agrees with the now well established data that rAAV.RPE65 gene therapy in the RPE65 dog model produces an improved visual response [16,21-23]. Although supporting the RPE65 dog ERG data, in this current study of rAAV.RPE65-injected *Rpe65*$^{-/-}$ mice it was difficult to determine the exact nature of the ERG response, and in particular whether it was rod and/or cone driven. In other studies performed on either untreated [7,13,40], 11-*cis* retinal-treated [41] or double mutant (*Rpe65*$^{-/-}$*Rho*$^{-/-}$, *Rpe65*$^{-/-}$*Cnga3*$^{-/-}$) *Rpe65*$^{-/-}$ mice [14], ERG responses have been attributed to both rods and cones. In the current work it is not possible to draw definitive conclusions as to whether the improved ERG responses seen is of rod, cone or a combined origin.

One of the interesting observations of this study was that the long-term changes in some retinal cells lasted well beyond measurable functional outcome. Electron microscopy indicated that the levels of lipid inclusions, an indicator of retinyl ester accumulation and halted visual cycle [7,22], was diminished in rAAV.RPE65-injected mice at 20 mo post-injection, suggesting that rAAV.RPE65 is still able to elicit a biological effect at these later time points. The remarkable recovery and long-term immunostaining of SWC-opsin in the functionally important cones suggests that cone function might be recoverable following rAAV.RPE65 gene therapy. However considering that the total number of photoreceptors continues to decrease, the restoration of SWC-opsin immunostaining may not necessarily represent protection against cone degeneration but only demonstrates the recovery of SWC-opsin in cones in the presence of an active visual cycle. Although these results were encouraging, ERG measurements were not able to differentiate between rod and cone function.

The transient improvement in ERG response, the decrease in lipid droplet accumulation and the positive SWC-opsin immunostaining upon rAAV.RPE65 administration were not accompanied by a statistically significant decrease in the rate of photoreceptor degeneration or apoptotic cell death. It appears, therefore, that the delivery of rAAV.RPE65, while being able to induce restarting of the visual cycle and phototransduction in the remaining photoreceptors in *Rpe65*$^{-/-}$ mice, was unable to slow or halt the photoreceptor degeneration that afflicts these mice. The finding of improved function without photoreceptor rescue is not unique, as a similar observation has been reported after subretinal injection of an rAAV encoding *Prph2* in a retinal degeneration slow mouse model [42,43]. Vision is maintained through the close and precise interaction between all the retinal cells. For example both in humans and in a transgenic mouse model for retinitis pigmentosa, the degeneration of rod photoreceptors eventually leads to the loss of cone photoreceptors as well [44]. At present one of the limitations of gene therapy is that only cells present within the retinal bleb can be targeted and within this treated region not all RPE cells undergo successful transduction and subsequent RPE65 production. The inability to restore the visual cascade in all RPE cells and hence the failure to restore function to the corresponding photoreceptors may be behind the lack of general photoreceptor rescue. In addition, the level and extent of RPE65 expression resulting from the rAAV.RPE65 injection might have been insufficient to support the survival of a significant number of functional photoreceptor cells. The restricted transduction area of subretinal rAAV injection, as seen from the confinement of transgene expression and reduction of lipid inclusion to RPE cells within the subretinal bleb, highlights the need to maximize both the efficiency of the rAAV construct delivery and the transgene expression *in vivo*. The efficiency of transgene delivery would be particularly important in diseases characterized by pan-retinal degeneration as they would presumably require the rAAV-mediated treatment to be present across the entire retina, ideally in every RPE cell in the retina.

A recent study in the RPE65 dog model, where the volume of virus that can be injected is not tightly restricted as in the small mouse eye, demonstrated that delivering larger volumes, and therefore higher titers of virus, gives a higher degree of functional rescue [21]. It may be, therefore, that the intensity of RPE65 expression is also important along with the size of the area being transduced, especially given the abundance of endogenous RPE65 protein in RPE cells of normal animals [45]. Fortunately rAAV biology, preparation, delivery and expression are being continuously improved [37,46-48] and no doubt future studies will see these limitations being overcome.

We performed our subretinal rAAV.RPE65 injections on *Rpe65*$^{-/-}$ mice immediately after weaning, that is, at 3 weeks of age. At this age there is no histological evidence of photoreceptor degeneration having started in the *Rpe65*$^{-/-}$ mice [7]. However, analysis of RPE65 expression

during embryogenesis and development has shown that rat RPE65 mRNA expression is detectable at E17 and protein at post natal days 4–5 [45,49]. If RPE65 expression commences so soon as to be visible in embryogenesis it is possible also that, in the absence of RPE65, the deleterious effects of RPE65 loss would also begin at this early stage. In other words, the cascade of events leading to eventual photoreceptor degeneration may be beginning at a much earlier age than our chosen age of injection. Thus, while rAAV.RPE65 expression can have a visual cycle effect within the time scale it is injected, introducing RPE65 expression alone at a later stage is insufficient to halt the photoreceptor degeneration cascade. If this hypothesis is true, the implications for rAAV-mediated gene therapy as a clinical option may be significant, as it may be essential to deliver rAAV.RPE65 at the time when RPE65 expression should be commencing in order to completely compensate for its loss. A recent article by [20] demonstrated that the early addition of 9-*cis* retinal caused a long-term reduction in lipids, and thus indicating that early intervention in LCA disease progression is potentially important. However, the feasibility of this approach from a clinical perspective is unclear. Genotypically, Rpe65 mutations are recessive and thus heterozygous parents may be unaware of their carrier status until they bear an *Rpe65*$^{-/-}$ homozygous child. Moreover, there is evidence that photoreceptor degeneration has already commenced before birth in fetuses afflicted with RPE65 mutations [50], suggesting that *in utero* delivery would be needed to fully prevent the effects of the RPE65 absence. In light of this information it is likely that neonatal treatment, even if performed soon after birth, may be only partially successful as a therapeutic option. Perhaps delivery of additional agents, either anti-apoptosis gene therapy [51,52], or oral retinoid supplements [18,20] may be needed to attain full disease prevention.

In conclusion, the data produced from this study demonstrated that subretinal injection of rAAV.RPE65 could produce a limited functional rescue of vision in *Rpe65*$^{-/-}$ mice. This functional rescue was seen in the form of an improved, albeit transient, ERG signal and a decreased level of lipid inclusions in treated eyes at later time points. In particular, the latter suggests that once optimized, rAAV may offer a long-term treatment option for LCA patients. Much work is still required, including improving our knowledge of the effects of RPE65 loss and the mechanisms that lead to the photoreceptor degeneration, as well as optimizing the timing, efficiency and specificity of the current rAAV gene technology. Although gene therapy on the *Rpe65*$^{-/-}$ mouse model may not have generated as much success as the dog model for LCA [16,21,22,53], the use of the *Rpe65*$^{-/-}$ mouse model has its merit in that it could be used in future studies to address how cones and rods are specifically affected by absence of RPE65 and to provide more information on the function of RPE65.

## Competing interests

None of the authors of this paper have competing interests.

## Authors' contributions

CML and MJTY prepared the clones and cesium chloride density gradient purified rAAV.RPE65, and designed, performed, analyzed and interpreted the data presented in Figs. 1, 4, 5, 6 and 7. MB performed the surgical procedures, NLB performed the ERG measurements and analysis of the data presented in Figs. 2 and 3. XZ prepared the heparin column purified rAAV.RPE65, TMR provided the *Rpe65*$^{-/-}$ mouse model, KN participated in the ERG data interpretation and PER provided the conceptual design of the project, initiated the collaborations and assisted in data analysis. All authors have had intellectual contribution to the preparation of this manuscript and have read and approved it.

## Acknowledgements

This project was financially supported by the Foundation for Fighting Blindness (USA), Retina Australia and the National Health and Medical Research Council (Australia). We thank Dr R. Samulski for the pSSV9 plasmid and Dr D. Zhang, Mr. B. Rae, Mr. S. Moore and Dr T. Robertson for their technical assistance and advice.

## References

1. Perrault I, Rozet JM, Gerber S, Ghazi I, Leowski C, Ducroq D, Souied E, Dufier JL, Munnich A, Kaplan J: **Leber congenital amaurosis.** *Mol Genet Metab* 1999, **68:**200-208.
2. Perrault I, Rozet JM, Ghazi I, Leowski C, Bonnemaison M, Gerber S, Ducroq D, Cabot A, Souied E, Dufier JL, Munnich A, Kaplan J: **Different functional outcome of RetGC1 and RPE65 gene mutations in Leber congenital amaurosis.** *Am J Hum Genet* 1999, **64:**1225-1228.
3. Dharmaraj SR, Silva ER, Pina AL, Li YY, Yang JM, Carter CR, Loyer MK, El-Hilali HK, Traboulsi EK, Sundin OK, Zhu DK, Koenekoop RK, Maumenee IH: **Mutational analysis and clinical correlation in Leber congenital amaurosis.** *Ophthalmic Genet* 2000, **21:**135-150.
4. Gu SM, Thompson DA, Srikumari CR, Lorenz B, Finckh U, Nicoletti A, Murthy KR, Rathmann M, Kumaramanickavel G, Denton MJ, Gal A: **Mutations in RPE65 cause autosomal recessive childhood-onset severe retinal dystrophy.** *Nat Genet* 1997, **17:**194-197.
5. Marlhens F, Bareil C, Griffoin JM, Zrenner E, Amalric P, Eliaou C, Liu SY, Harris E, Redmond TM, Arnaud B, Claustres M, Hamel CP: **Mutations in RPE65 cause Leber's congenital amaurosis.** *Nat Genet* 1997, **17:**139-141.
6. Lorenz B, Gyurus P, Preising M, Bremser D, Gu S, Andrassi M, Gerth C, Gal A: **Early-onset severe rod-cone dystrophy in young children with RPE65 mutations.** *Invest Ophthalmol Vis Sci* 2000, **41:**2735-2742.
7. Redmond TM, Yu S, Lee E, Bok D, Hamasaki D, Chen N, Goletz P, Ma JX, Crouch RK, Pfeifer K: **Rpe65 is necessary for production of 11-cis-vitamin A in the retinal visual cycle.** *Nat Genet* 1998, **20:**344-351.
8. Saari JC: **Retinoids in photosensitive systems.** *Retinoids in Photosensitive systems.* Edited by: Sporn MB, Roberts AB and Goodmans DS. New York, Raven Press Ltd; 1994:351-384.
9. Rando RR: **The biochemistry of the visual cycle.** *Chem Rev* 2001, **101:**1881-1896.
10. Wrigstad A, Narfstrom K, Nilsson SE: **Slowly progressive changes of the retina and retinal pigment epithelium in Briard dogs**

**with hereditary retinal dystrophy. A morphological study.** *Doc Ophthalmol* 1994, **87:**337-354.
11. Aguirre GD, Baldwin V, Pearce-Kelling S, Narfstrom K, Ray K, Acland GM: **Congenital stationary night blindness in the dog: common mutation in the RPE65 gene indicates founder effect.** *Mol Vis* 1998, **4:**23.
12. Veske A, Nilsson SE, Narfstrom K, Gal A: **Retinal dystrophy of Swedish briard/briard-beagle dogs is due to a 4-bp deletion in RPE65.** *Genomics* 1999, **57:**57-61.
13. Ekesten B, Gouras P, Salchow DJ: **Ultraviolet and middle wavelength sensitive cone responses in the electroretinogram (ERG) of normal and Rpe65 -/- mice.** *Vision Res* 2001, **41:**2425-2433.
14. Seeliger MW, Grimm C, Stahlberg F, Friedburg C, Jaissle G, Zrenner E, Guo H, Reme CE, Humphries P, Hofmann F, Biel M, Fariss RN, Redmond TM, Wenzel A: **New views on RPE65 deficiency: the rod system is the source of vision in a mouse model of Leber congenital amaurosis.** *Nat Genet* 2001, **29:**70-74.
15. Narfstrom K, Wrigstad A, Ekesten B, Nilsson SE: **Hereditary Retinal Dystrophy in the Briard Dog: Clinical and Hereditary Characteristics.** *Veterinary & Comparative Ophthalmology* 1994, **4:**85-92.
16. Acland GM, Aguirre GD, Ray J, Zhang Q, Aleman TS, Cideciyan AV, Pearce-Kelling SE, Anand V, Zeng Y, Maguire AM, Jacobson SG, Hauswirth WW, Bennett J: **Gene therapy restores vision in a canine model of childhood blindness.** *Nat Genet* 2001, **28:**92-95.
17. Wrigstad A, Nilsson SE, Narfstrom K: **Ultrastructural changes of the retina and the retinal pigment epithelium in Briard dogs with hereditary congenital night blindness and partial day blindness.** *Exp Eye Res* 1992, **55:**805-818.
18. Van Hooser JP, Aleman TS, He YG, Cideciyan AV, Kuksa V, Pittler SJ, Stone EM, Jacobson SG, Palczewski K: **Rapid restoration of visual pigment and function with oral retinoid in a mouse model of childhood blindness.** *Proc Natl Acad Sci U S A* 2000, **97:**8623-8628.
19. Gouras Peter, Kong Jian, Tsang Stephen H.: **Retinal Degeneration and RPE Transplantation in Rpe65-/- Mice.** *Invest. Ophthalmol. Vis. Sci.* 2002, **43:**3307-3311.
20. Van Hooser JP, Liang Y, Maeda T, Kuksa V, Jang GF, He YG, Rieke F, Fong HK, Detwiler PB, Palczewski K: **Recovery of visual functions in a mouse model of Leber congenital amaurosis.** *J Biol Chem* 2002, **277:**19173-19182.
21. Ford M, Bragadottir R, Rakoczy PE, Narfstrom K: **Gene transfer in the RPE65 null mutation dog: relationship between construct volume, visual behavior and electroretinographic (ERG) results.** *Doc Ophthalmol* 2003, **107:**79-86.
22. Narfstrom K, Katz ML, Bragadottir R, Seeliger M, Boulanger A, Redmond TM, Caro L, Lai CM, Rakoczy PE: **Functional and structural recovery of the retina after gene therapy in the RPE65 null mutation dog.** *Invest Ophthalmol Vis Sci* 2003, **44:**1663-1672.
23. Narfstrom K, Katz ML, Ford M, Redmond TM, Rakoczy E, Bragadottir R: **In vivo gene therapy in young and adult RPE65-/- dogs produces long-term visual improvement.** *J Hered* 2003, **94:**31-37.
24. Rolling F, Shen WY, Tabarias H, Constable I, Kanagasingam Y, Barry CJ, Rakoczy PE: **Evaluation of adeno-associated virus-mediated gene transfer into the rat retina by clinical fluorescence photography.** *Hum Gene Ther* 1999, **10:**641-648.
25. Redmond TM, Hamel CP: **Genetic analysis of RPE65: from human disease to mouse model.** *Methods Enzymol* 2000, **316:**705-724.
26. Rolling F, Samulski RJ: **AAV as a viral vector for human gene therapy. Generation of recombinant virus.** *Mol Biotechnol* 1995, **3:**9-15.
27. Zolotukhin S, Byrne BJ, Mason E, Zolotukhin I, Potter M, Chesnut K, Summerford C, Samulski RJ, Muzyczka N: **Recombinant adeno-associated virus purification using novel methods improves infectious titer and yield.** *Gene Ther* 1999, **6:**973-985.
28. Rakoczy PE, Sarks SH, Daw N, Constable IJ: **Distribution of cathepsin D in human eyes with or without age-related maculopathy.** *Exp Eye Res* 1999, **69:**367-374.
29. Bennett J, Maguire AM, Cideciyan AV, Schnell M, Glover E, Anand V, Aleman TS, Chirmule N, Gupta AR, Huang Y, Gao GP, Nyberg WC, Tazelaar J, Hughes J, Wilson JM, Jacobson SG: **Stable transgene expression in rod photoreceptors after recombinant adeno-associated virus-mediated gene transfer to monkey retina.** *Proc Natl Acad Sci U S A* 1999, **96:**9920-9925.
30. Bainbridge JW, Mistry A, Schlichtenbrede FC, Smith A, Broderick C, De Alwis M, Georgiadis A, Taylor PM, Squires M, Sethi C, Charteris D, Thrasher AJ, Sargan D, Ali RR: **Stable rAAV-mediated transduction of rod and cone photoreceptors in the canine retina.** *Gene Ther* 2003, **10:**1336-1344.
31. Shen WY, Lai CM, Lai YK, Zhang D, Zaknich T, Sutanto EN, Constable IJ, Rakoczy PE: **Practical considerations of recombinant adeno-associated virus-mediated gene transfer for treatment of retinal degenerations.** *J Gene Med* 2003, **5:**576-587.
32. Sarra GM, Stephens C, Schlichtenbrede FC, Bainbridge JW, Thrasher AJ, Luthert PJ, Ali RR: **Kinetics of transgene expression in mouse retina following sub-retinal injection of recombinant adeno-associated virus.** *Vision Res* 2002, **42:**541-549.
33. Scharfmann R, Axelrod JH, Verma IM: **Long-term in vivo expression of retrovirus-mediated gene transfer in mouse fibroblast implants.** *Proc Natl Acad Sci U S A* 1991, **88:**4626-4630.
34. Loser P, Jennings GS, Strauss M, Sandig V: **Reactivation of the previously silenced cytomegalovirus major immediate-early promoter in the mouse liver: involvement of NFkappaB.** *J Virol* 1998, **72:**180-190.
35. Chen WY, Townes TM: **Molecular mechanism for silencing virally transduced genes involves histone deacetylation and chromatin condensation.** *Proc Natl Acad Sci U S A* 2000, **97:**377-382.
36. Gaetano C, Catalano A, Palumbo R, Illi B, Orlando G, Ventoruzzo G, Serino F, Capogrossi MC: **Transcriptionally active drugs improve adenovirus vector performance in vitro and in vivo.** *Gene Ther* 2000, **7:**1624-1630.
37. Malik AK, Monahan PE, Allen DL, Chen BG, Samulski RJ, Kurachi K: **Kinetics of recombinant adeno-associated virus-mediated gene transfer.** *J Virol* 2000, **74:**3555-3565.
38. Shen WY, Lai YK, Lai CM, Rakoczy PE: **Impurity of recombinant adeno-associated virus type 2 affects the transduction characteristics following subretinal injection in the rat.** *Vision Res* 2004, **44:**339-348.
39. Rabinowitz JE, Rolling F, Li C, Conrath H, Xiao W, Xiao X, Samulski RJ: **Cross-packaging of a single adeno-associated virus (AAV) type 2 vector genome into multiple AAV serotypes enables transduction with broad specificity.** *J Virol* 2002, **76:**791-801.
40. Rohrer B, Goletz P, Znoiko S, Ablonczy Z, Ma JX, Redmond TM, Crouch RK: **Correlation of regenerable opsin with rod ERG signal in Rpe65-/- mice during development and aging.** *Invest Ophthalmol Vis Sci* 2003, **44:**310-315.
41. Ablonczy Z, Crouch RK, Goletz PW, Redmond TM, Knapp DR, Ma JX, Rohrer B: **11-cis-retinal reduces constitutive opsin phosphorylation and improves quantum catch in retinoid-deficient mouse rod photoreceptors.** *J Biol Chem* 2002, **277:**40491-40498.
42. Ali RR, Sarra GM, Stephens C, Alwis MD, Bainbridge JW, Munro PM, Fauser S, Reichel MB, Kinnon C, Hunt DM, Bhattacharya SS, Thrasher AJ: **Restoration of photoreceptor ultrastructure and function in retinal degeneration slow mice by gene therapy.** *Nat Genet* 2000, **25:**306-310.
43. Sarra GM, Stephens C, de Alwis M, Bainbridge JW, Smith AJ, Thrasher AJ, Ali RR: **Gene replacement therapy in the retinal degeneration slow (rds) mouse: the effect on retinal degeneration following partial transduction of the retina.** *Hum Mol Genet* 2001, **10:**2353-2361.
44. Naash MI, Hollyfield JG, al-Ubaidi MR, Baehr W: **Simulation of human autosomal dominant retinitis pigmentosa in transgenic mice expressing a mutated murine opsin gene.** *Proc Natl Acad Sci U S A* 1993, **90:**5499-5503.
45. Hamel CP, Tsilou E, Harris E, Pfeffer BA, Hooks JJ, Detrick B, Redmond TM: **A developmentally regulated microsomal protein specific for the pigment epithelium of the vertebrate retina.** *J Neurosci Res* 1993, **34:**414-425.
46. Brument N, Morenweiser R, Blouin V, Toublanc E, Raimbaud I, Cherel Y, Folliot S, Gaden F, Boulanger P, Kroner-Lux G, Moullier P, Rolling F, Salvetti A: **A versatile and scalable two-step ion-exchange chromatography process for the purification of recombinant adeno-associated virus serotypes-2 and -5.** *Mol Ther* 2002, **6:**678-686.
47. Schneider H, Muhle C, Douar AM, Waddington S, Jiang QJ, von der Mark K, Coutelle C, Rascher W: **Sustained delivery of therapeutic concentrations of human clotting factor IX--a compari-**

**son of adenoviral and AAV vectors administered in utero.** *J Gene Med* 2002, **4:**46-53.
48. Weber M, Rabinowitz J, Provost N, Conrath H, Folliot S, Briot D, Cherel Y, Chenuaud P, Samulski J, Moullier P, Rolling F: **Recombinant adeno-associated virus serotype 4 mediates unique and exclusive long-term transduction of retinal pigmented epithelium in rat, dog, and nonhuman primate after subretinal delivery.** *Mol Ther* 2003, **7:**774-781.
49. Manes G, Leducq R, Kucharczak J, Pages A, Schmitt-Bernard CF, Hamel CP: **Rat messenger RNA for the retinal pigment epithelium-specific protein RPE65 gradually accumulates in two weeks from late embryonic days.** *FEBS Lett* 1998, **423:**133-137.
50. Porto FB, Perrault I, Hicks D, Rozet JM, Hanoteau N, Hanein S, Kaplan J, Sahel JA: **Prenatal human ocular degeneration occurs in Leber's congenital amaurosis (LCA2).** *J Gene Med* 2002, **4:**390-396.
51. Liang FQ, Dejneka NS, Cohen DR, Krasnoperova NV, Lem J, Maguire AM, Dudus L, Fisher KJ, Bennett J: **AAV-mediated delivery of ciliary neurotrophic factor prolongs photoreceptor survival in the rhodopsin knockout mouse.** *Mol Ther* 2001, **3:**241-248.
52. Petrin D, Baker A, Coupland SG, Liston P, Narang M, Damji K, Leonard B, Chiodo VA, Timmers A, Hauswirth W, Korneluk RG, Tsilfidis C: **Structural and functional protection of photoreceptors from MNU-induced retinal degeneration by the X-linked inhibitor of apoptosis.** *Invest Ophthalmol Vis Sci* 2003, **44:**2757-2763.
53. Narfstrom K, Bragadottir R, Redmond TM, Rakoczy E, van Veen T, Brunn A: **Functional and structural evaluation after AAV.RPE65 gene transfer in the canine model of leber's congenital amaurosis.** *Retinal Degenerations Mechanisms and Experimental Therapy Volume 533*. Edited by: JG Hollyfield RE Anderson MM La Vail. New York: USA., Kluwer Academic / Plenum Publishers; 2003:423-430.